Supporting Information

Kalwa et al. 10.1073/pnas.1320854111

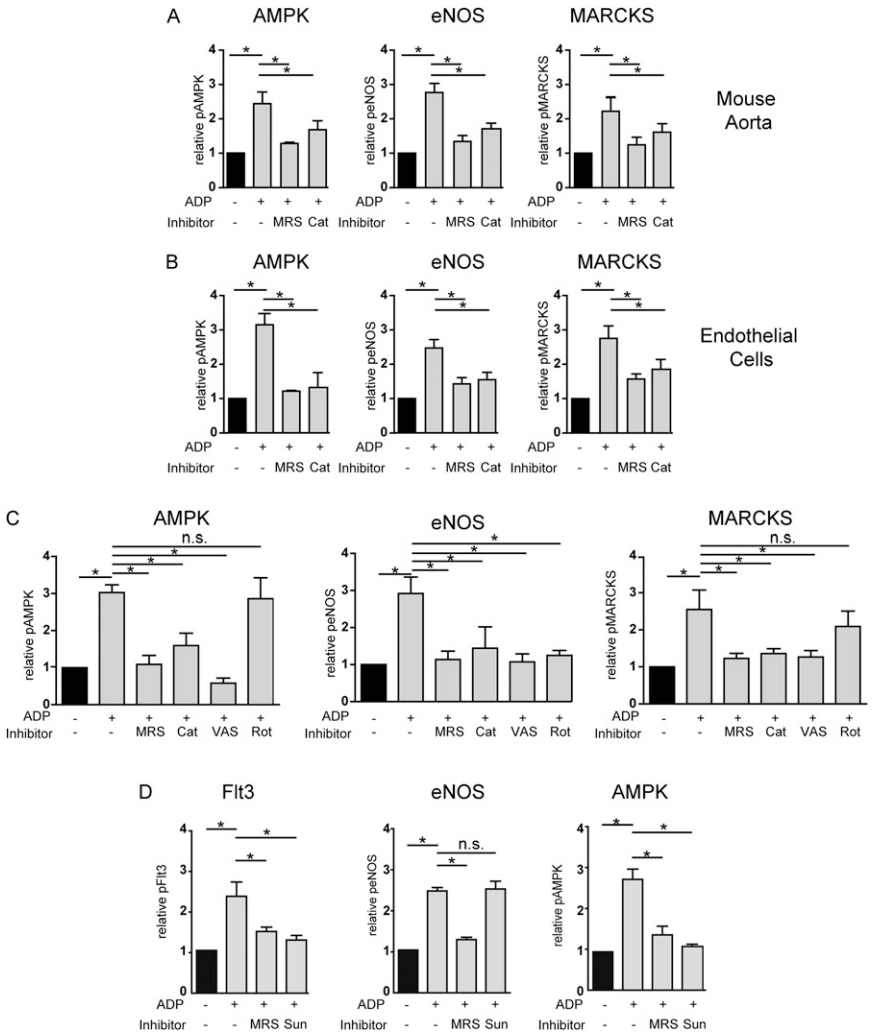

Fig. S1. Statistical analyses of pooled data from immunoblot experiments. *A* and *B* show pooled data from four independent experiments identical in design to the representative immunoblots shown in Fig. 1*B*, in which murine aortic preparations (*A*) or cultured endothelial cells (*B*) were incubated with ADP in the presence or absence of the P2Y1-specific blocker MRS2179 or the cell-permeant H_2O_2-catabolizing enzyme PEG-catalase. *C* shows pooled data from three identically configured experiments corresponding to the representative immunoblots shown in Fig. 5, in which endothelial cells were incubated with MRS2179, PEG-catalase, the NADPH oxidase inhibitor VAS2870, or the mitochondrial inhibitor rotenone and treated with ADP. *D* shows pooled data corresponding to the representative immunoblots shown in Fig. 6*B*, in which endothelial cells were incubated with ADP in the presence or absence of MRS2179 or the receptor tyrosine kinase inhibitor sunitinib ($n = 3$ identical experiments) and probed with total and phosphospecific antibodies as shown; $^*P < 0.05$ (ANOVA).

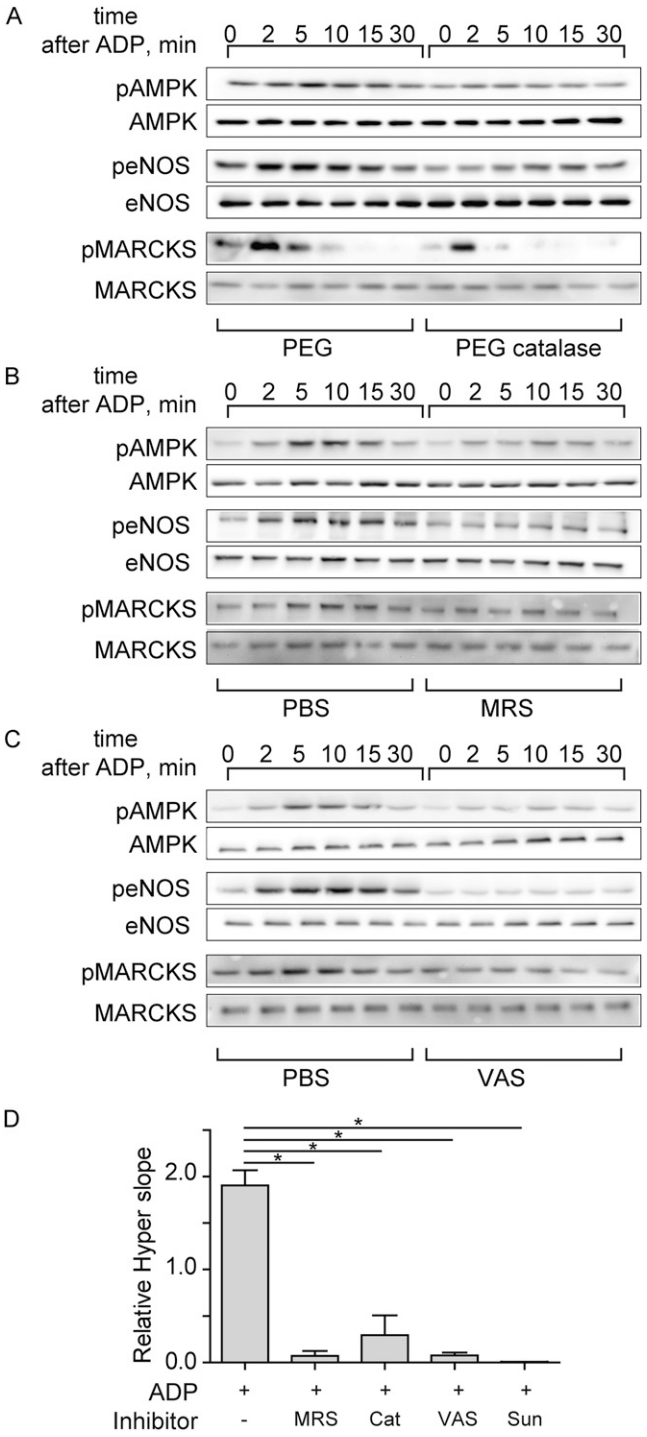

Fig. S2. Effects of PEG-catalase, MRS2179, sunitinib, and VAS2870 on ADP-mediated phosphorylation and HyPer2 responses in cultured endothelial cells. *A–C* show a time-response analysis of ADP-induced protein phosphorylation in endothelial cells. Cells were incubated with ADP (50 μM) for the indicated times in the presence or absence of PEG-catalase, MRS2179, or VAS2870. Membranes were probed with phosphospecific and total antibodies directed against eNOS, AMPK, and MARCKS. The results shown are representative of four identical experiments that yielded similar results. *D* shows the effects of these same inhibitors on ADP-stimulated HyPer2 responses. Endothelial cells transfected with the HyPer2 plasmid were treated with ADP (50 μM) in the presence of absence of PEG-catalase, MRS2179, sunitinib, or VAS2870 and then analyzed by ratiometric imaging of the HyPer2 signal; the slope of the ratiometric response following addition of ADP was calculated and is presented in this figure ($n = 3$; $^*P < 0.05$ by ANOVA).

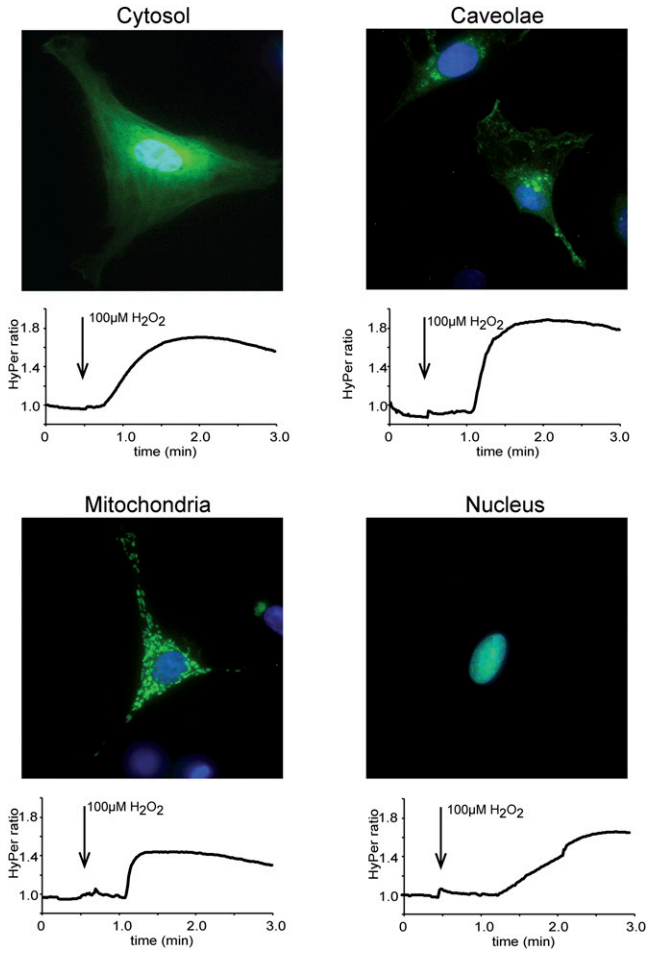

Fig. S3. Detection of hydrogen peroxide levels by differentially targeted variants of HyPer2. Shown are representative photomicrographs and quantitative live-cell time course experiments in endothelial cells transfected with differentially targeted variants of the hydrogen peroxide specific biosensor HyPer2 expressed in cytosol (CYTO), caveolae (CAV), nucleus (NUC), or mitochondria (MITO), as indicated, and then treated with H_2O_2. The cytosolic, nuclear, and mitochondria-targeted HyPer2 constructs were from Evrogen. The caveolae-targeted HyPer2 was generated by amplifying the cytosolic HyPer2 coding sequence (minus its initial ATG) by PCR, using as forward primer 5′-GATCTCTGCAAGCCAGCAGGGCGAGACGA; reverse primer 5′-CTAGATTAAACCGCCTGTTTTAAAACTTTATCG; this fragment was ligated in frame with the N-terminal sequence of eNOS extending from the initial eNOS ATG to the BglII site at base pair 1520 (*Bos taurus* eNOS cDNA M89952).